

INVESTIGATING PYROCLASTIC VOLCANISM IN THE TAURUS-LITTROW VALLEY (TLV) USING THE STATION 3 DOUBLE DRIVE TUBE 73001-73002. C.K. Shearer^{1,2}, S.B. Simon¹, J. Dottin³, M. Cato¹, F.M. McCubbin⁴, R.A. Zeigler⁴, J. Gross⁴, P. Lucey⁵, L. Sun⁵, J.I. Simon⁴, H.H. Schmitt⁶, B.L. Jolliff⁷, S. Eckley⁴, L. Borg⁸, B. Jacobsen⁸, M. D. Dyar^{9,10}, C.R. Neal^{10,11}, and the ANGSA science team¹², ¹Dept. of Earth and Planetary Science, Institute of Meteoritics, University of New Mexico, Albuquerque, New Mexico 87131; ²Lunar and Planetary Institute, Houston TX 77058; ³Carnegie Institute of Washington, Washington, DC 20005; ⁴ARES, NASA Johnson Space Center, Houston TX 77058-3696; ⁵University of Hawaii at Manoa, Honolulu, HI 96822; ⁶University of Wisconsin-Madison, P.O. Box 90730, Albuquerque NM 87199; ⁷Washington University in St. Louis, St. Louis, MO 63130; ⁸Lawrence Livermore National Laboratory, Livermore, CA 94550; ⁹Dept. of Astronomy, Mount Holyoke College, South Hadley MA 01075; ¹⁰Planetary Science Institute, Tucson, AZ 85719; ¹¹University of Notre Dame, Notre Dame IN 46556; ¹²ANGSA Science Team list at <https://www.lpi.usra.edu/ANGSA/teams/>. (cshearer@unm.edu) (cshearer@unm.edu)

Introduction: Well over 100 pyroclastic deposits have been identified on the Moon [1]. Eruptive processes such as represented by these deposits transported endogenous volatiles from the Moon's mantle to its surface. Debris from pyroclastic deposits has been identified in all Apollo and Luna samples. The high-Ti pyroclastic deposit sampled at Shorty Crater by the Station 4 double drive tube (74001-74002) is our best sampling of these types of deposits [2]. Samples 78500 and 78526 [3-5], NAC images of fissures in the Sculptured Hills [3-4], ash identified in 70001-7 [4,6], and other green volcanic glass [7,8] indicate that very low-Ti basalt (VLT) eruptions also occurred in TLV. The double drive tube core being investigated by the ANGSA initiative provides another view of TLV pyroclastic eruptions. The regolith in 73001-73002 and the regolith breccias therein have numerous pyroclastic beads. Some individual regolith breccia fragments have abundant pyroclastic beads (>50 in a polished surface). In this work, we address the following questions. Do these glass beads overlap in composition with those sampled elsewhere in the TLV or do they record another episode of pyroclastic eruption? Are the magmas associated with pyroclastic eruptions petrogenetically related to the crystalline mare basalts in the TLV? Finally, is the volatile record of the pyroclastic eruptions better preserved in the newly opened and specially contained Station 3 double drive tube core?

73001-73002 pyroclastic bead samples: Volcanic beads examined for this study were derived from the ≤ 1 mm size fraction of the 73001-73002 core. Splits from the core were sieved into several size fractions and mounted into circular polished thin sections. Additional pyroclastic beads were identified in regolith breccia fragments (>4 mm) that were separated from the 73001-73002 core during Preliminary Examination (PE). These lithic fragments were imaged by micro-XCT at the Johnson Space Center. Samples considered in this study include lithic fragments 64C (73002,466), 1133A (73002,454), and 227 (73001,528,529).

Analytical Strategy: Sample splits from the less than 1 mm size fraction from core samples 73001-73002 were selected throughout the stratigraphy of the double drive tube. They were sieved into distinct size fractions at the

University of New Mexico. Grains from each sample and size fraction were mounted on 1-inch circular slides and polished. A subset of these samples was allocated to D. Dyar for FTIR and x-ray absorption analyses for H distribution, and Fe valence state measurements. Individual pyroclastic beads from the sieved samples and regolith breccias were imaged and analyzed by SEM and EPMA

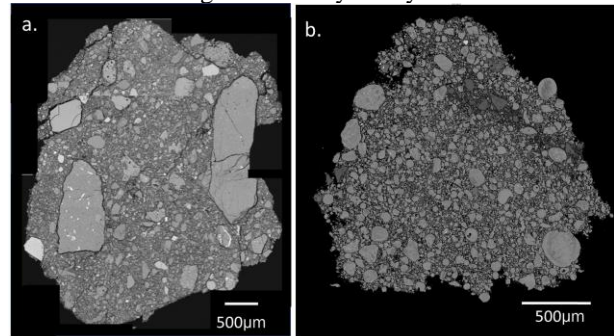


Figure 1. Backscattered electron (BSE) lithic fragments containing pyroclastic beads. a. 64C. b. 227.

at the University of New Mexico. For glass beads, multiple point analyses were carried out at bead cores and rims. In devitrified beads with fine-grained olivine+ilmenite+chromite, bulk analyses were carried out with broad beam or rastered beam analyses. Once fully documented, glasses will be analyzed for trace components using SIMS, nano-SIMS, and LA-ICP-MS

Morphology of pyroclastic beads: In the samples examined, pyroclastic beads range in size from 10 μ to 450 μ m. Most are between 45-150 μ m in diameter. A higher proportion of the smaller droplets (<45 μ m) are broken. Most of the beads are spherical in morphology, and there appears to be a very limited number of fused, compound beads. The beads range from completely glassy to highly devitrified (Fig. 2). The devitrified mineralogy is olivine + ilmenite \pm chromite \pm metal (Fig. 2d). Initial imaging has identified Na- and K-bearing chlorides. It is highly uncertain whether these are pristine lunar in origin. If terrestrial, this could be contamination during sample preparation.

Composition of pyroclastic beads: The dominant pyroclastic bead compositions observed correspond to those

of high-Ti orange and black glasses. We are in the process of estimating the proportions of orange to black within the lithic fragments and in the regolith of the core. In Figure 3 (Mg' versus TiO_2), the high-Ti beads plot at higher Mg' than the crystalline mare basalts from the TLV. The one anomalous point is being further investigated to confirm its uniqueness. In addition, the orange-black beads overlap with the various high-Ti glass types found at Station 4 previously identified by [7,8] as high-Ti type 1, high-Ti type 2, and high Ti type 74220. Compositions also plot along potential liquid-lines-of-descent [8,9].

In addition to the high-Ti volcanic beads, VLT glasses were identified. Initial analyses indicate that these glasses have higher Mg' and slightly higher TiO_2 than either the VLT glass identified by [7,8] and glass associated with Station 8 rake sample 78526 [5] (Fig. 3).

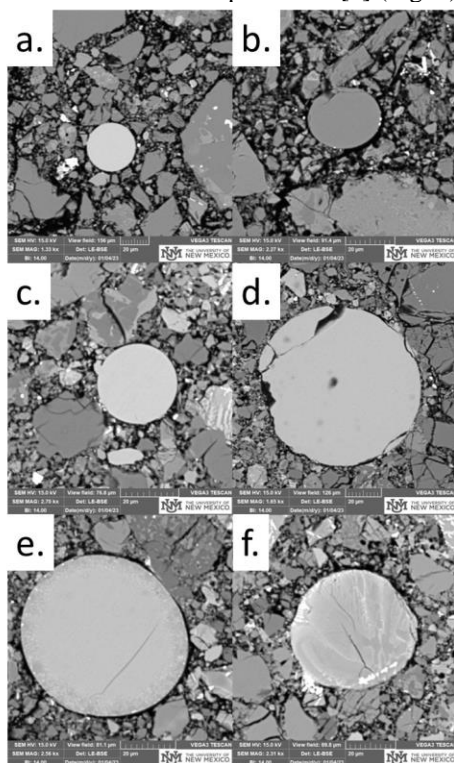


Figure 2. a. High-Ti orange glass bead B4 from lithic fragment 64C. b. Feldspathic glass bead B8 from 64C. Most likely impact in origin. c. High-Ti orange glass bead B3 from 1133A. d. Orange glass bead from 1133A. e. Orange glass bead with devitrified rim of olivine and ilmenite from 1133A. f. High-Ti black bead BSDV from 1133A, consisting of glass, olivine and ilmenite.

Conclusions: Several conclusions can be reached based on these preliminary observations: (1) There is a low proportion of compound droplets in the 73001-73002 core. This could be a product of the landslide process which was detrimental to the preservation of this form. Alternatively, the lack of compound droplets may be at-

tributed to a stage in the pyroclastic eruption [10]. Morphology of ilmenite, Cr-rich spinel, and olivine in devitrified glasses will aid in the interpretation of cooling histories. (2) There are potentially some Na- and K-chloride compounds preserved in these new samples. This should be further explored. In addition to chloride compounds on surfaces and in fractures, these specially curated samples may provide additional information on lunar volatiles and should be analyzed by Nano-SIMS and other approaches. (3) The high-Ti beads in the core represent the three glass compositions previously documented [7,8]. Some of the volcanic beads in the core represent melts that lie along liquid-lines-of-descent from these three melt compositions. There appears to be other high-Ti bead compositions that are distinct. Do these beads closely represent parental melts to the crystalline mare basalts? Trace element analyses of specific elements and elemental ratios will answer this question (e.g., La vs Yb, Co/Sc vs Cr/La) [11]. (4) The VLT glass beads thus far analyzed are more primitive (higher Mg') than other VLT glasses analyzed from the TLV [7,8]. The Mg' of these VLT glasses overlap with the VLTs from Apollo 15 (glass B and C). Are these compositions representing parental melts to the other VLTs from the TLV? More likely, it appears that a number of distinct VLT magmas may have erupted from fissures in the TLV[2-4].

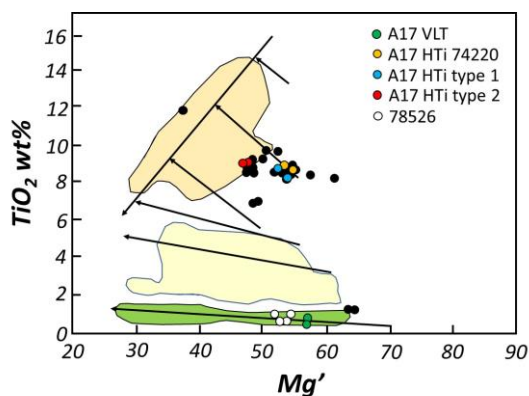


Figure 3. TiO_2 versus Mg' for orange, black, and green pyroclastic beads from 73001-73002. Data also presented for distinct pyroclastic bead types from Apollo 17 [7,8] and sample 78526. Superimposed on diagram are fields for VLT, low, intermediate, and high-Ti crystalline basalts [8] and liquid-lines-of-descent calculated by [3] from Longhi [9].

References: [1] Gustafson J. et al. (2012). *JGR: Planets*, 117(E12). [2] Schmitt H. (2017 LPSC XLVIII, abst.# 1072. [3] Schmitt H. (2023) pers. Com. [4] Schmitt H. et al. (2017). *Icarus*, 298, 2-33. [5] Warner J. et al. (1979). *UNM Spec. Publ.* #20, 20 pp. [6] Vaniman D. et al. (1978) LPSC IX, 1185-1227. [7] Delano J. (1986). *JGR: Solid Earth*, 91(B4), 201-213. [8] Shearer C. et al. (2006). *RiMG*, 60, 365-518. [9] Longhi J. (1992). *GCA* 56, 2235-2251. [10] Heiken G. & McKay D. (1977). *PLSC* 8th, 3243-3255. [11] Shearer et al. (2023). *RiMG* 87, in press.